NJC

Accepted Manuscript

This article can be cited before page numbers have been issued, to do this please use: S. Zheng, S. Xu, J. Zhou, R. Shen, Y. Ji, M. Shen and W. Li, *New J. Chem.*, 2018, DOI: 10.1039/C7NJ04958G.

ROYAL SOCIETY OF CHEMISTRY

rsc.li/njc

View Article Online
DOI: 10.1039/C7NJ04958G

Journal Name

ARTICLE

Insight into the Claisen condensation of methyl acetate and dimethyl carbonate to dimethyl malonate

Received 00th January 20xx,
Accepted 00th January 20xx

DOI: 10.1039/x0xx00000x

www.rsc.org/

Sainan Zheng,[a] Shiwei Xu,[a] Jinghong Zhou,[a,*] Rongchun Shen,[a] Yang Ji,[b] Ming Shen,[c] and Wei Li[a,#]

Mechanistic study on the synthesis of dimethyl malonate (DMM) via condensation of methyl acetate (MA) and dimethyl carbonate (DMC), catalyzed by sodium methoxide, has been conducted using gas chromatography-mass spectrometry, liquid chromatography-electrospray ionization- mass spectrometry, X-ray diffraction, solid-state nuclear magnetic resonance spectroscopy and density functional theory calculations. The results indicated that Claisen condensation of MA and DMC in the presence of methoxide yielded $(CH_3OCO)_2CHNa$ (DMNa) instead of DMM since the DMM is easily deprotonated by the methoxide catalyst. Further protonation after the condensation by adding proton-donor reagent is essential to obtain DMM. Based on the experimental results, a detailed reaction mechanism for the condensation of MA and DMC into DMM in the presence of methoxide has been proposed and disclosed by computational calculations. Besides, it has been proven that the base strength of the catalyst has critical effect on the condensation reaction and the DMM yield.

1. Introduction

1,3-Propanediol (1,3-PDO) has versatile commercial applications for many industries, particularly for polymer and composites industries,[1-3] which led to a dramatically expanding demand for 1,3-PDO in last decade. 1,3-PDO is conventionally produced via two petroleum pathways: acrolein hydration by the Degussa process[4] and ethylene oxide hydroformylation by the Shell process[5]. Recently, glycerol hydrogenolysis[6-8] and microbial production[9-10] have been reported as alternatives for 1,3-PDO production. Although some of these processes have been commercialized to the scale of ten thousand tons, the current productivity of 1,3-PDO is far from its rapidly expanding global market.[9] Many efforts therefore have been made to explore new processes of high yield, low cost, less pollution, and easy to industrialize.

More recently, we have proposed a new alternative for 1,3-PDO synthesis through hydrogenation of dimethyl malonate (DMM) from Claisen condensation of syngas-derived chemicals, methyl acetate (MA) and dimethyl carbonate (DMC). MA is currently produced from esterification of acetic acid and methanol[11] or carbonylation of methanol with CO[12], while DMC is commonly produced by the oxidative carbonylation of methanol[13-14], both tracking back to methanol which is definitely produced from syngas. In addition, the abundant productivities and the low prices of MA and DMC make them excellent feedstock for synthesizing 1,3-PDO. This new process consists of two steps. First, methyl acetate (MA) reacts with dimethyl carbonate (DMC) through Claisen condensation to give dimethyl malonate (DMM)[15], then DMM is hydrogenated to 1,3-PDO via a catalytic vapor-phase process[16-17]. Our preliminary results has demonstrated for the first time that DMM of *ca.* 70% yield could be achieved by Claisen condensation of MA and DMC, employing sodium methoxide as a catalyst. Also, the further hydrogenation of DMM into 1,3-PDO over a Cu/SiO_2 catalyst has successfully produced 1,3-PDO with 42% yield.

As a potential route for 1,3-PDO large-scale production, this novel process demands more understanding, among which the synthesis of intermediate DMM is of most importance. To the best of our knowledge, the mechanism of Claisen condensation between MA and DMC, as well as the role of the catalyst, remain unrevealed. Therefore, insights into the chemistry of this condensation reaction will definitely provide instrumental fundamentals for catalyst design and process optimization.

Here in this work, we report a mechanistic study on the condensation of MA and DMC, focusing on the role of methoxide catalysts. The products under different reaction conditions have been extensively analyzed by gas chromatography-mass spectrometry (GC-MS), liquid chromatography-electrospray ionization- high-resolution mass spectrometry (LC/ESI-HRMS), X-ray diffraction (XRD), solid-state nuclear magnetic resonance spectroscopy (SS-NMR) to enlighten the reaction pathways during condensation. Moreover, a detailed reaction mechanism of the condensation

[a] *School of Chemical Engineering, East China University of Science and Technology, 130 Meilong Road, Shanghai 200237, China.*
[b] Shanghai Pujing Chemical Industry Co. Ltd, 1305 Huajing Road, Shanghai 200231, China.
[c] *Shanghai Key Laboratory of Magnetic Resonance, East China Normal University, 3663 Northern Zhongshan Road, Shanghai 200062, China*
Electronic Supplementary Information (ESI) available: [details of any supplementary information available should be included here]. See DOI: 10.1039/x0xx00000x

View Article Online
DOI: 10.1039/C7NJ04958G

has been proposed based on the reaction results combining with the density functional theory (DFT) calculation results.

2. Experimental

2.1 Materials and reaction procedure.

MA, DMC, DMM, and dimethyl sulfoxide (DMSO) (>99.0% purity by GC analysis) were dried with 5A molecular sieves to water content less than 0.005% determined by coulometric Karl Fisher titration. Sodium methoxide (CH_3ONa) and potassium methoxide (CH_3OK) solutions in DMSO were titrated using literature methods[18]. All the reactions were conducted in a 250 mL bath-type flask under nitrogen (99.999%) at ambient pressure. Gas-tight syringes were employed to transfer moisture-sensitive solutions.

Typically, the condensation of MA and DMC catalyzed by sodium methoxide was carried out as follows: solution of 5.4 g CH_3ONa dissolved in 50 mL DMSO was introduced to the flask which has been pre-charged with N_2 at an ambient pressure, then the flask was placed in an oil-bath. After the system reached the reaction temperature (typically 341 K), MA/DMC (14.8 g /90 g) solution (which has been pre-heated to the reaction temperature) was introduced into the reactor by a gas-tight syringe, and the reaction was initiated instantly with vigorous stirring. After 12 h, the reaction was instantly terminated by cooling the reactor to room temperature (RT) in iced water and stood still for 12 h before analyzing. The liquid products were analyzed by gas chromatography (GC 9560, Shanghai Huaai) equipped with an FID detector and a DB-200 capillary column (30 m×0.32 mm×0.25 μm). The same experiment were carried out at least in triplicate for each run to make sure the relative error was <5%.

2.2 Product characterization.

GC-MS system consisted of an Agilent 7890A gas chromatograph and an Agilent 7863B auto injector coupled with an Agilent 5975C mass selective detector. The mass spectral scan rate was 2.86 scan s^{-1}. The GC was operated in splitless injection mode with a helium (ultra-high purity, 99.999%) flow rate of 0.7 mL min^{-1} and the injection volume was 1 μL. The MS was operated in the electron ionization (EI) mode with an ionization voltage of 70 eV and a source temperature of 503 K. The GC-MS chromatographic separations were carried out on a HP-5 capillary column (30 m×0.25 mm × 0.25 μm).

Liquid chromatography-electrospray ionization- high resolution mass spectrometry (LC/ESI-HRMS) measurements were carried out on a Shimadzu LCMS-8030 triple quadrupole mass spectrometer connected to a Shimadzu LC-20AD chromatograph (Kyoto, Japan). The ionization was performed under normal electrospray conditions (flow rate: 4 ml min^{-1}, 4.5 kV, dry temperature: 473 K) in positive mode. Methanol (Merck LCMS Grade) was adopted as the mobile phase, and samples were diluted with methanol at a ratio of 1:80 (V/V) before analysis and the injection volume was set at 5 μL.

The XRD measurements were carried out using a Rigaku C/max-2500 diffraectometer employing the Cu Kα radiation (λ=1.5406 Å) with a scanning angle (2ϑ) range of 5-80°. Samples were carefully dried with a vacuum dryer under nitrogen (99.999%) before testing.

Solid-state ^{13}C NMR spectra were recorded on a Bruker AVANCE-III 9.4 T (^{13}C Larmor frequency of 100 MHz) spectrometer at room temperature. Samples were packed into a 4.0 mm rotor and were spinning at 8 kHz. ^{1}H-^{13}C cross-polarization (CP) was employed with radio-frequency field of $\pi/2$ and contact pulse optimized on Glycine sample. All spectra were obtained with 2 s recycle delay, a contact time of 4 ms, and two-pulse phase modulation ^{1}H decoupling. The chemical shifts were referenced to tetramethylsilane by using glycine as an external reference.

2.3 Computational methods.

All electronic structure simulation calculations were performed with the Gaussian 09 program package[19] using its default criteria. Ab initio density functional B3LYP were employed with a standard 6-31+G (d) basis set using the PCM solvent model[20]. Optimal structures at B3LYP/6-31+G (d) theory level of each transition state and intermediate are demonstrated in Fig. S1. Frequency calculations were carried out for all stationary points at the same level of theory as the geometry optimization. No imaginary vibrational frequencies were acquired for all local minimum structures, while only one single imaginary frequency was presented for the transition state that corresponded to the expected motion along the reaction coordinate. Single-point calculations at the MP2/6-31+G(d) level for the optimized structures were then carried out incorporating thermal corrections to Gibbs free energy as achieved at the B3LYP/6-31+G(d) level of theory and PCM corrections for dimethyl sulfoxide (DMSO) as the solvent (ΔG, 298.15 K, 1.0 atm).

3. Results and discussion

3.1 The protonation for DMM formation after the condensation.

The condensation reaction of MA and DMC in DMSO solution was conducted under 341 K for 12 h, then cooled to RT immediately and stood still for 12 h. The reacted system split into 2 phases-a white solid phase and a translucent liquid phase, as demonstrated in Fig. S2 (A). Sampling of the liquid phase was analyzed by a GC-MS spectrometer and only unreacted MA, DMC, and newly-formed methanol were detected besides the solvent DMSO. Surprisingly, the expecting product DMM has not been examined (refer to the GC-MS spectra in Fig. S3 (A)).

Since methanol, as one of the condensation products, has been confirmed in the product mixture, it is natural to speculate that the condensation did occur in the reaction system. And another expecting product of condensation probably exist in certain form. Thus acetic acid (HAc), H_2O, and HCl acid, serving as proton-donors, were introduced into the reaction system after the condensation reaction in order to extract the objective product DMM. Interesting phenomena were observed that the reaction system turned into a white solid phase and a transparent organic liquid phase when HAc

View Article Online
DOI: 10.1039/C7NJ04958G

Table 1 Chemical composition of separated liquid phases under various post-treatment conditions

Post-treatment reagent	Liquid phase composition	
	Aqueous phase	Oil phase[a]
-	-	MA, DMC, CH_3OH
HAc	-	HAc, MA, DMC, CH_3OH, DMM
H_2O	H_2O[a], MeOH[a], NaOH	MA, DMC, CH_3OH, DMM
HCl	H_2O[a], MeOH[a], NaCl	MA, DMC, CH_3OH, DMM

Reaction conditions: DMC/MA/CH_3ONa = 10/2/1 mol/mol/mol, reaction temperature = 341 K, reaction time = 12 h.
[a] Determined by GC-MS analyses.

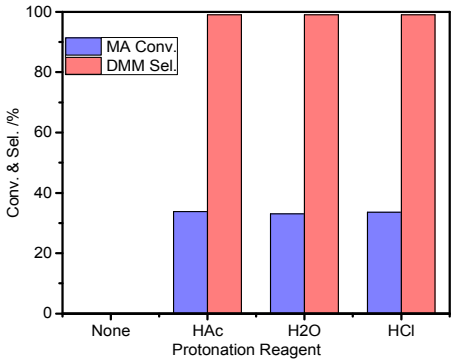

Fig. 1 Effect of post-treatment reagent on the condensation reaction. Reaction conditions: DMC/MA/CH_3ONa = 10/2/1 (mol/mol/mol), T = 341 K, reaction time = 12 h.

==========

was the proton donor, and that 2 liquid phases, an aqueous and an oil phase were observed when H_2O or HCl as the proton-donor (see to Fig. S2 (C) & (D), respectively). The composition of all the liquid phases were determined by GC-MS (Fig. S3) and summarized in Table 1. It can be seen that the objective product DMM existed in the oil-phase for all these three cases. It is worth noting that identical reaction results determined by quantitative GC, i.e. 33% conversion of MA and 100% selectivity of DMM as shown in Fig. 1, were obtained for the three proton-donor solvents.The existence of DMM was confirmed in the oil phase of the condensation mixtures only after protonation of the reaction system, which suggests that DMM may be transformed into a solid compound and mixed with the catalyst sodium methoxide. To reveal the composition of the solid phase after condensation, the organic compounds was removed from the mixture of the condensation by drying under N_2 at 463 K for 24 h, then the remained white solid was processed with HAc at RT. The HAc-treated solution was analyzed and at last the DMM was detected as expected. This indicates that DMM does remain as a solid phase with sodium methoxide and it could have been transformed to a sodium salt of DMM, which may be ascribed to the deprotonation of DMM by CH_3ONa.

For further understanding the deprotonation of DMM by CH_3ONa, we investigated the CH_3ONa-mediated deprotonation of DMM in DMSO. The reaction of CH_3ONa/DMSO solution and

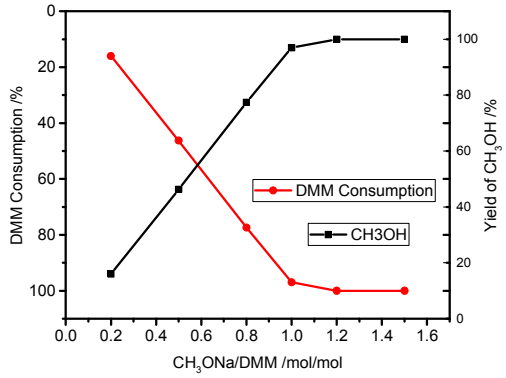

Fig. 2 Consumption of DMM in DMSO with addition of sodium methoxide at 341 K.

==========

pure DMM was conducted at 341 K for 12 h with the CH_3ONa/DMM molar ratio ranged from 0.1 to 1.5. As illustrated in Fig. 2, when the ratio was below 1.0, DMM consumption increased linearly with the addition of CH_3ONa yielding equimolar methanol, indicating DMM was deprotonated by CH_3ONa. After CH_3ONa/DMM molar ratio reached 1.0, DMM consumption remained unchanged since the consumption had been 100%. After the deprotonation of DMM by CH_3ONa, the solution was added with D_2O and analyzed by GC-MS to reveal the location of deprotonated hydrogen. The GC-MS spectrum (Fig. S4) clearly showed a strong peak at *m/z* of 102.1 belonging to $[CH_3OCOCHDCO]$ fragments, while *m/z* of 101 belonging to $[CH_3OCOCH_2CO]$ fragments in the standard mass spectra of dimethyl malonate, indicating that D has coordinated with α-C of $[(CH_3OCO)_2CH]$-species generating $(CH_3OCO)_2CHD$. These observations strongly support a conclusion that deprotonation of DMM by equimolar of CH_3ONa to give methanol and a sodium malonate whose formation has not been reported previously. Here we presumably describe the sodium malonate as $(CH_3OCO)_2CHNa$ (denoted as DMNa).

Reversed-phase liquid chromatography-electrospray ionization-high resolution mass spectrometry (LC/ESI-HRMS) has been widely used for qualitative analysis of molecular formulas because of the high mass resolution of HRMS[21-22]. To investigate the formation of DMNa further, LC/ESI-HRMS analysis on the CH_3ONa-mediated DMM solution was performed, and the result is displayed in Fig. S5. A strong peak at *m/z* of 155.0319 in the mass spectrum can be observed. According to the ChemOffice 2015, theoretical *m/z* value of $[(CH_3OCO]_2CH_2^+Na]^+$ fragment is 155.03148. Here in this case, the peak at 155.0319 can be assigned to the $[(CH_3OCO]_2CH_2^+Na]^+$ fragment with a mass accuracy of 2.71 ppm. This result indicates the cleavage between α-C and α-H bond of DMM and the coordination of the Na ion. This LC/ESI-HRMS result provides further evidence for the formation of the DMNa species. Hence, the reaction between DMM and sodium methoxide can be described as eq 1.

$$(CH_3OCO)_2CH_2 + CH_3ONa \rightarrow (CH_3OCO)_2CHNa + CH_3OH \quad (1)$$

View Article Online
DOI: 10.1039/C7NJ04958G

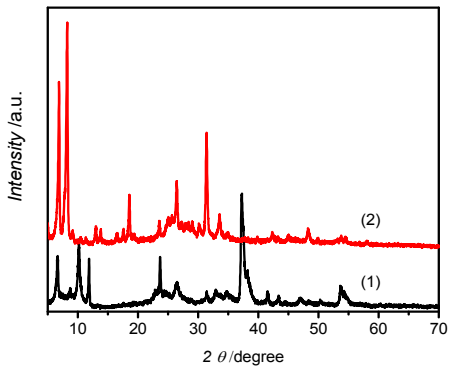

Fig. 3 XRD profiles of (1) CH_3ONa and (2) DMNa.

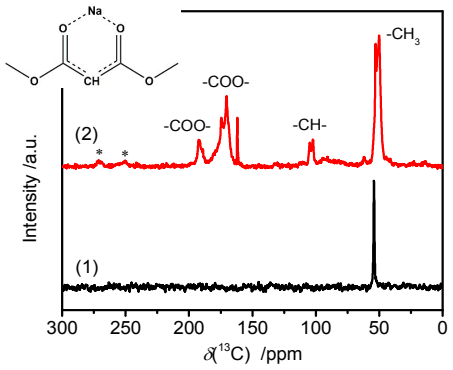

Fig. 4 ^{13}C CP MAS NMR spectra of (1) CH_3ONa and (2) DMNa. Inset: Structure of DMNa.

Note: Spinning sidebands are denoted with asterisks (*). Sharp resonance at 161 ppm may corresponds to DMM which was formed due to the contact with H_2O in air during the sample handling procedure.

==========

To examine the existence of DMNa further, after the reaction of CH_3ONa and DMM with a molar ratio of 1.0, the reaction system was dried in nitrogen at 453 K for 24 h to remove the organic and yielded white salt in powder. Then the nature of the salt was then characterized by XRD. Fig. 3 presents the XRD patterns of both DMNa salt and CH_3ONa. The characteristic peaks at 2ϑ = 6.64, 8.70, 10.16, 11.86, 24.36, 26.28, 37.28, and 53.64° are ascribed to CH_3ONa (JCPDS 19-1876)[23]. After protonation of DMM with CH_3ONa, the characteristics at 2ϑ = 6.88, 8.24, 18.56, 26.44, 31.42, 33.58, and 48.34° arise and the diffraction peaks belonging to CH_3ONa diminished, inferring that DMNa is the major DMM-bearing species in the reaction system during the condensation reaction.

In addition, the yielded powder was analyzed by SS-NMR. The SS-NMR results show that there should be minor component of unreacted CH_3ONa in the reaction product, as there is negligible overlap of methyl signal ($-CH_3$) around 50 ppm (Fig. 4). Although we cannot preclude the existence of unreacted DMM, the broad feature of resonance at 51, 103, 172, and 192 ppm should imply the ^{13}C-^{23}Na coupling which cannot be decoupled with current equipment. Besides, the surprisingly high frequency signal of carboxylic (-COO-) and secondary (-CH-) carbon signal also indicates the possible conjugated effect in the six-membered ring. Thus, the structure of DMNa can be identified as the inset picture in Fig. 4.

Conclusively, combining the GC-MS, LC/ESI-HRMS, XRD, and SS-NMR results, we believe that the absence of DMM after Claisen condensation of MA and DMC is due to the deprotonation of DMM to $(CH_3OCO)_2CHNa$ by the catalyst sodium methoxide. Thus, further protonation after the condensation is essential to obtain DMM.

3.2 Reaction mechanism and the role of methoxide.

When carboxylic esters containing an α-H are treated with a strong base, such as sodium ethoxide, a condensation occurs to give β-keto ester via an enolate anion. This reaction is called Claisen condensation[24]. According to experimental results in Section 3.1, a tentative mechanism of Claisen condensation between MA and DMC catalyzed by methoxide is proposed as Scheme 1.

As illustrated in Scheme 1, the condensation of MA and DMC can be divided into the four stages: (1) MA with an α-H is deprotonated by the catalyst, take sodium methoxide as an example, leading to the formation of an enolate anion (enolate A); (2) enolate A nucleophilically attacks the carbonyl carbon of dimethyl carbonate, generating the intermediate; (3) the alkoxy group departs from the intermediate generating DMM; (4) the newly formed α-H of DMM is removed by the catalyst to give a new resonance-stabilized enolate salt (DMNa). In addition, DMNa is the resulting product rather than DMM in the methoxide-catalyzed reaction.

To disclose the proposed mechanism more closely, we conducted theoretical computations for the condensation model employing 1 equiv of MA and 1 equiv of DMC in DMSO with sodium methoxide as a catalyst. A series of geometries for reactants, intermediates, and transition structures were

==========

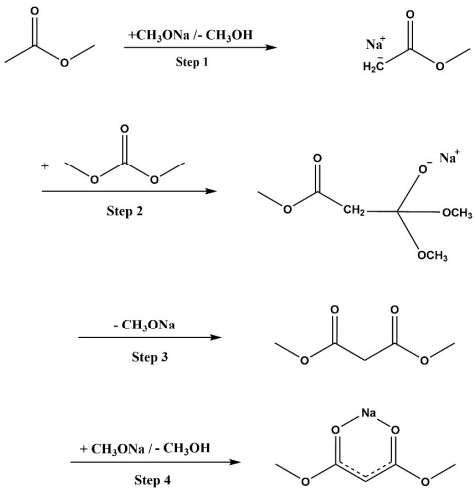

Scheme 1 Reaction Pathway for the condensation of MA and DMC in the presence of sodium methoxide.

View Article Online
DOI: 10.1039/C7NJ04958G

Table 2 MP2/6-31+G(d) computed activation Gibbs energy and Gibbs free energy values along the reaction profiles of the condensation reaction*.

Reaction steps	CH_3ONa		CH_3OK	
	$\Delta G^{\ddagger}$ (kJ mol^{-1})	ΔG_r (kJ mol^{-1})	$\Delta G^{\ddagger}$ (kJ mol^{-1})	ΔG_r (kJ mol^{-1})
Step 1	89.4	51.8	75.8	34.2
Step 2	100.6	220.1	105.8	13.4
Step 3	32.4	4.4	37.5	3.2
Step 4	21.3	-70.7	17.8	-65.3

* $\Delta G^{\ddagger}$ and ΔG_r denote the activation Gibbs energy and Gibbs free energy values for each elementary reaction in the condensation of methyl acetate and dimethyl carbonate to dimethyl malonate catalyzed by CH_3ONa and CH_3OK in DMSO, respectively.

==========

investigated, and the optimized structures of transition structures and intermediates are demonstrated in Fig. S1. Specially, the calculated structure of DMNa (Fig. S1 (F)) displays a planar six-membered ring, in which Na coordinates with two carbonyl oxygen atoms; it is in good agreement with the experimental identification of DMNa structure by SS-NMR (Fig. 4).

After the confirmation of the lowest energy pathway for the condensation reaction of MA and DMC catalyzed by CH_3ONa, the calculated standard Gibbs energy of activation ($\Delta G^{\ddagger}$) and the Gibbs free energy (ΔG_r) for each elementary reaction during condensation are listed in Table 2. As can be seen in Table 2, the initial step of the condensation reaction is the deprotonation of MA by the catalyst CH_3ONa via the transition TS1 (Fig. S1 (A)) forming a nucleophile compound, $-CH_2COOCH_3$ (enolate A) and methanol simultaneously, whose activation Gibbs energy is 89.4 kJ·mol^{-1}. The subsequent step is the attack of enolate A to DMC forming a tetrahedral intermediate with the activation free energy of 100.6 kJ mol^{-1}. Next, the tetrahedral intermediate undergoes the departure of the $-CH_3$ group to give sodium methoxide and DMM, requiring an activation energy of 32.4 kJ mol^{-1}. Finally, the product DMM is further deprotonated to its enolate salt by CH_3ONa and at the same time alcohol yields with an activation energy of 21.3 kJ mol^{-1}, which is much lower than all the three preceding steps. This analysis of activation Gibbs energy along the reaction coordination shows a highest value for the addition reaction and a lowest activation Gibbs energy for DMM deprotonation which means the addition step is the rate-determining step, and the reaction between DMM and CH_3ONa is in a chemical equilibrium, indicating the consumption of DMM by deprotonated to DMNa upon its formation is kinetically favoured. Besides, the concentration of DMM in solution can be derived from the Gibbs free energy of DMM deprotonation (ΔG_r = -70.7 kJ mol^{-1}), depicting DMM is prone to be totally converted into DMNa thermodynamically. Therefore, no free DMM can be detected in the system, which has been already verified in our experimental results in Table 1 and Fig. 2.

3.3 The effect of base strength on DMM formation.

According to the DFT calculation results on the reaction of MA and DMC catalyzed by CH_3ONa and CH_3OK, shown in Table 2, the deprotonation of MA by the catalysts is crucial for the

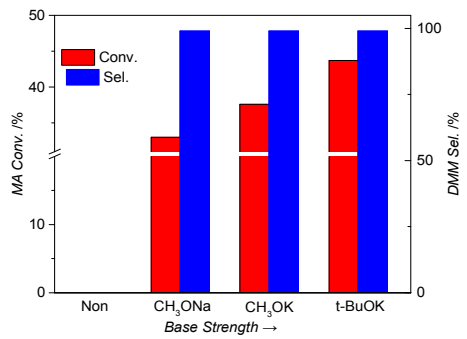

Fig. 5 Influences of base strength of catalysts on their catalytic behaviors for the condensation of methyl acetate and dimethyl carbonate.

Reaction conditions: DMC/MA/catalyst = 10/2/1 (mol/mol/mol), T = 341 K, reaction time = 12 h. Post-protonated by HAc.

==========

condensation, and its activation barrier is significantly affected by the alkali strength of the catalyst.

To evaluate the effect of alkali strength of catalysts on the reaction, the condensation of MA and DMC was carried out with CH_3Ona,CH_3OK, and potassium t-butoxide (t-BuOK). The catalytic results after deprotonation with HAc are presented in Fig. 5. It can be seen that DMM is the main product with a selectivity of 100% for all the three alkali catalysts and MA conversion increases from ca. 33% to ca. 44% when the base changes from CH_3ONa to t-BuOK. This indicates that high alkali strength facilitates the conversion of MA, which is in line with the DFT computation results in Table 2.

As the computational calculations shown, the Gibbs free energy gets notably smaller (from 51.8 kJ mol^{-1} to 34.2 kJ mol^{-1}) for the deprotonation of MA when the catalyst changes from CH_3ONa to CH_3OK, indicating higher catalyst alkali strength favor the equilibrium of the MA deprotonation to enolate A.

For the addition of enolate A to DMC, the rate-determining step, the Gibbs free energy reduces from 220.1 kJ mol^{-1} to 13.4 kJ mol^{-1}, indicating the formation of DMM is favoured thermodynamically when the catalyst changes from CH_3ONa to CH_3OK. Besides, in comparison with Na ion, the larger size of K may lead to it being better coordinated by the oxygen atoms of acryl group and α-C. This may allow K to mediate the deprotonation and coordinate with C=O in DMC more effectively, which could explain why potassium methoxide demonstrates better catalytic performances for the condensation of MA and DMC than sodium methoxide.

4. Conclusions

Experimental and DFT studies were carried out to elucidate the mechanism of DMM synthesis from the Claisen condensation of MA and DMC catalyzed by methoxide catalyst. The condensation products were extensively characterized by GC-MS, LC-ESI/HRMS, XRD, and SS-NMR. The results indicated that in the presence of sodium methoxide the expecting

View Article Online
DOI: 10.1039/C7NJ04958G

condensation product, DMM, is deprotonated of its α-H to sodium malonate whose chemical structure has been experimentally identified through combined characterizations for the first time. Moreover, the subsequent computational calculation has also proven that the methoxide not only initiated the deprotonation of MA to proceed condensation, but also triggered the deprotonation of objective DMM to DMNa. Therefore, the protonation after condensation is a necessity to obtain DMM product. In a more general view, this insight into the Claisen condensation provides useful fundamentals for synthesizing β-keto esters from α-H esters which can be potentially derived via syngas route.

Conflicts of interest

There are no conflicts to declare.

Acknowledgements

We gratefully acknowledge the support from by the National Natural Science Foundation of China (21376076), and we thank the help of Prof. Dr. Bingwen Hu in NMR measurements.

References

1 Kurian, J. V., J. *Polym Environ*, 2005, **13**, 159.
2 J. Ma, W. Yu, M. Wang, X. Jia, F. Lu, J. Xu, *Chin. J. Catal.*, 2013, **34**, 492-507.
3 U. Witt, R. J. Muller, J. Augusta, *Macromol Chem Phys*, 1994, **195**, 793.
4 F. R. Lawrence, R. H. Sullivan. US Patent 3687981, 1972.
5 J. C. Sullivan, *Ullmann's Encyklopedia of Industrial Chemistry*, John Wiley and Sons, Inc., Weinheim, 1993, pp. 163-171.
6 J. Wang, N. Lei, C. Yang, Y. Su, X. Zhao, A. Wang, *Chin. J. Catal.*, 2016, **37**, 1513.
7 L. Niu, R. Wei, H. Yang, X. Li, F. Jiang, G. Xiao, *Chin. J. Catal.*, 2013, **34**, 2230.
8 C. Deng, L. Leng, J. Zhou, X. Zhou, W. Yuan, *Chin. J. Catal.*, 2015, 3**6**, 1750.
9 R. K. Saxena, P. Anand, S. Saran, J. Isar, *Biotechnol Adv.,* 2009, **27**, 895.
10 G. Yang, J. Tian, J. Li, *Appl Microbiol Biotechnol.*, 2007, **73**, 1017.
11 R. Rönnback, T. Salmi, A. Vuori, H. Haario, J. Lehtonen, A. Sundqvist, E. Tirronen, *Chem. Eng. Sci.*, 1997, **52**, 3369.
12 Fengbo Li, Bingfeng Chen, Zhijun Huang, Tao Lu, Yin Yuan and Guoqing Yuan, *Green Chem.*, 2013, **15,** 1600.
13 U. Romano, R. Tesel, M. M. Mauri, P. Rebora, *Ind. Eng. Chem. Prod. Res. Dev.*, 1980, **19**, 396.
14 G. Fiorani, A. Perosa, M. Selva, *Green Chem.*, 2018, **20**, 288.
15 X. Wang, W. Li, R. Shen, *Natural Gas Chemical Industry*, 2016, **41**, 38.
16 S. Zhao, J. Chen, B. Zhang, J. Yang, S. Zheng, W. Li, *Natural Gas Chemical Industry*, 2016, **41**, 10.
17 S. Zheng, K. Zhu, W. Li, Y. Ji, *New J. Chem.*, 2017, **41**, 5752.
18 J. F. Bunnett, G. T. Davis, H. Tanida, *J. Am. Chem. Soc.*, 1962, **84**, 1606
19 M. J. Frisch, G. W.Trucks, H. B. Schlegel, et al. Gaussian 09, Reversion A.1; Gaussian Inc., Wallingford, CT, 2009.
20 C. S. Pomelli, J. Tomasi, *J. Phys. Chem. A*, 1997, **101**, 3564.
21 E. N. Fung, Y. Xia, A. Aubry, J. Zeng, T. Olah, M. Jemal, J. Chromatogr. B, 2011, **879**, 2919.
22 M. Zhu, L. Ma, H. Zhang, W. G. Humphreys, Anal. Chem., 2007, **79**, 8333.
23 K. Chandrran, R. Nithya, K. Sankaran, A. Gopalan, V. Ganesan, *Bull. Mater. Sci.*, 2006, **29**, 173.
24 M. B. Smith, J. March, *March's Advanced Organic Chemistry*, Wiley-Interscience, Davers, 2007, 1452-1455.

View Article Online
DOI: 10.1039/C7NJ04958G

Contents Entry

Insight into the Claisen condensation of methyl acetate and dimethyl carbonate to dimethyl malonate

Sainan Zheng[a], Shiwei Xu[a], Jinghong Zhou[a,*], Rongchun Shen[a], Yang Ji[b], Ming Shen[c], Wei Li[a,#]

[a] *School of Chemical Engineering, East China University of Science and Technology, 130 Meilong Road, Shanghai 200237, China*

[b] *Shanghai Pujing Chemical Industry Co. Ltd, 1305 Huajing Road, Shanghai 200231, China*

[c] *Shanghai Key Laboratory of Magnetic Resonance, East China Normal University, 3663 Northern Zhongshan Road, Shanghai 200062, China*

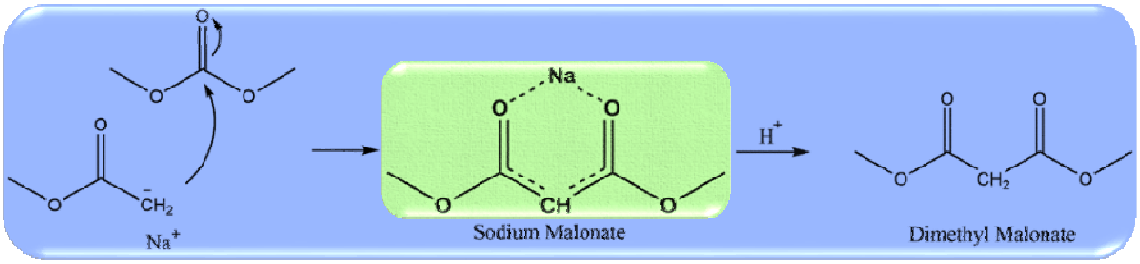

A mechanistic model for Claisen condensation of methyl acetate and dimethyl carbonate in the presence of sodium methoxide to sodium malonate and further protonation to dimethyl malonate is proposed based on experimental and computational results.